The 2017 World Congress on
Advances in Structural Engineering and Mechanics (ASEM17)
28 August - 1 September, 2017, Ilsan(Seoul), Korea

Experimental and numerical study on flush-repaired composite laminates under compressive load

*Xingming Zhang[1)], Yuanpei Lan[1)], and Jifeng Xu[2)]

Beijing Key Laboratory of Civil Aircraft Structures and Composite Materials, Beijing Aeronautical Science & Technology Research Institute, Future Science and Technology Park, Changping District, Beijng, China, 102211
[2)] xujifeng@comac.cc

ABSTRACT

Experimental study was conducted to investigate the failure mode and strength behavior of flush-repaired composite laminates with damage under compressive load, and the results were then compared with those from the experiments on virgin laminates without any damage. The failure mode of flush-repaired composite laminate specimens was local buckling, and that for virgin laminate specimens was global buckling. Since thick covering layer resulted in higher local buckling loads at repaired region compared with those at non-repaired region, hence as a result, the local buckling at non-repaired region occurred first and led to the final failure. In addition, experimental results show that flush-repaired composite laminates usually recover well under compressive load, and the repaired laminates have better post-buckling load-carrying capability than the virgin laminates.

Furthermore, a finite element model of flush-repaired composite laminates under compressive load was established. 3D Hashin failure criteria was adopted to identify the damages of laminates on both patch and covering layers, and zero-thickness cohesive elements was used between layers to simulate inter-laminar damage. The failure modes obtained from finite element analysis conform to the experimental results. Due to the complexity of the design and process of flush-repair, the failure loads of the flush-repaired composite laminates is not easy to be obtained through numerical simulation to exactly match with those from experiment. However, in this study their small difference meets the fidelity requirement for engineering applications. Therefore, the proposed finite element model is able to anticipate the failure mode and failure load of flush-repaired composite laminates under compressive load.

1) Engineer.
2) Senior Technical Fellow and Deputy Chief Designer.

1. INTRODUCTION

Composite material content indicates progressiveness of civil aircraft. With wide application of composite structure, composite structure damage repair technology becomes key point for new generation civil aircraft safe operation, and for fighting for civil aircraft market share (Peng 2008). Flush-repair is a frequently used method, which can recover well structure behavior and satisfy aerodynamic shape requirement at the same time. Therefore, many researchers investigated properties and analysis method of flush-repaired composite structures under different loads (Guo2012).

Campilh (2007) studied the tensile strength and failure mode of flush-repaired composite laminates, Guo (2012) performed tensile behavior of double side flush-repaired composite laminates, Zhu (2012) brought about a progressive damage analysis 3-D finite element model for stepped-patch repaired laminates under tensile load, Liu (2013) investigated the tensile strength of flush-repaired composite laminates with penetration damage by experimental and finite element analysis, Peng (2016) analyzed the tensile property of flush-repaired skin and panel in a practical case. While Lan (2014) researched the failure load and failure mode of flush-repaired composite laminates under shear load with experimental and finite element analysis. Besides, Soutis (2000) performed simulation analysis of the failure mode for flush-repaired composite laminates under compressive load, Yu (2008) researched the compressive strength of flush-repaired composite structures, and Xu (2011) investigated the stability of stepped-patch repaired stiffened panel under compressive load.

In this study, experiments were performed on composite laminates with damage and virgin laminates specimens under compressive load to investigate the failure mode and strength recovery ratio. Then 3-D finite element mode of flush-repaired composite laminates under compressive load was established, the simulation results of which were validated by the experimental results.

2. EXPERIMENT

Rectangular composite laminates were used in the experiments, the lay-up of the base laminate was $[45/0/-45/90]_{2S}$, and the test area was 350mm×250mm with a loading frame of 60mm. A hole was machined at the base laminates center to simulate non-penetrating damage, while the diameter of the hole was 15mm and thickness was half of the composite laminates. The scarf angle was 1:30, and the patch dimension was calculated from ply thickness, scarf angle and the ply number. The patch prepreg was laid-off by automatic blanking machine, to insure the ply orientation of the patch was consistent with the base laminates. The lay-up of covering layers was [45/0/-45] from inside to outside with three plies in total.

The base laminates and patches were prepared with X850 composite material, then the base laminates and patches were adhesive bonded by binder (JII6B). The mechanical properties of X850 and J116B were listed in Table 1 and Table 2 (Lan 2014).

Table 1 Mechanical properties of X850 laminates

E_{11}/GPa	E_{22}/GPa	E_{33}/GPa	G_{12}/GPa	G_{23}/GPa	G_{13}/GPa	v_{12}
168.50	10.30	10.30	6.21	3.00	6.21	0.33
v_{23}	v_{13}	X_t/MPa	X_c/MPa	Y_t/MPa	Y_C/MPa	S/MPa
0.3	0.33	2785.6	1071.3	74.8	332.9	120.9

Note: E_{11}, E_{22}, E_{33}—Young's moduli in the principal directions; G_{12}, G_{23},G_{13}—shear moduli in the principal directions; v_{12}, v_{23}, v_{13}—Poisson's ratios in the principal directions; X_t—Tensile strength in 1 direction; X_c—Compressive strength in 1 direction; Y_t—Tensile strength in 2 direction; Y_c—Compressive strength in 2 direction; S—shear strength.

Table 2 Mechanical properties of J116B adhesive

E/GPa	G/GPa	v	*Shear stress*/MPa	*Peel stress*/MPa	h/mm
1	0.385	0.3	24.5	7.5	0.2

Note: E—Young's modulus; G—shear modulus; v—Poisson's ratios; h—thickness.

Three composite flush-repaired laminate specimens were prepared, and numbered FY-1, FY-2, FY-3. Meanwhile, three virgin composite laminate specimens were prepared too for comparison, and numbered WY-1, WY-2, WY-3.

Strain gages were lapped on specimens to detect whether the load distribution was reasonable during the loading process, and the failure loads were confirmed through strain-load curves. Each specimen was arranged to have 10 strain gages with distinct number for each of them to be recognized, and the gages numbered 1 to 5 were distributed on the front side (repaired face), and those numbered 101 to 105 were distributed on the back side (Fig. 1).

Special fixture was developed for the experiments. Specimens were placed in the fixture to keep specimens borders parallel to the bottom face of the fixture, and to contact well with the test platform. Tool steels were fastened by bolts on left and right sides of specimens with symmetry, avoiding premature instability. Griped composite flush-repaired laminate specimen for compressive load experiment is shown in Fig. 2.

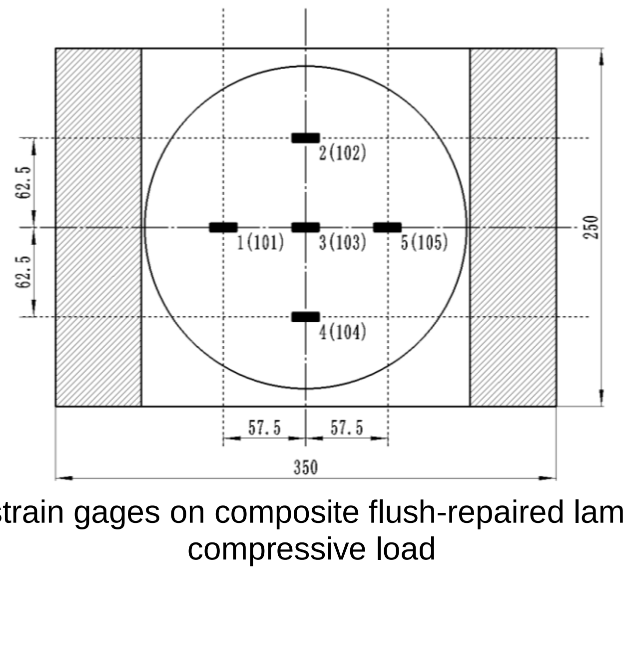

Fig. 1 Distribution of strain gages on composite flush-repaired laminate specimen under compressive load

The specimens were loaded by stages, with a 2mm/min loading rate. The loading process include three stages: first, applying 0% to 30% estimate ultimate load and then the loading process was stopped to check the loading condition, connection of fixture with specimen and equipment, and to test machine operation, strain measure and data collection system to make sure they were working normally. Furthermore, specimens should not experience permanent deformation after unloading. Second, applying 0% to 30% estimate ultimate load on specimens again, ensuring related measure data was consistent with the first time. Thirdly, loading up to the ultimate load, the initial and final failure load as well as failure mode, and correlation measure data were recorded.

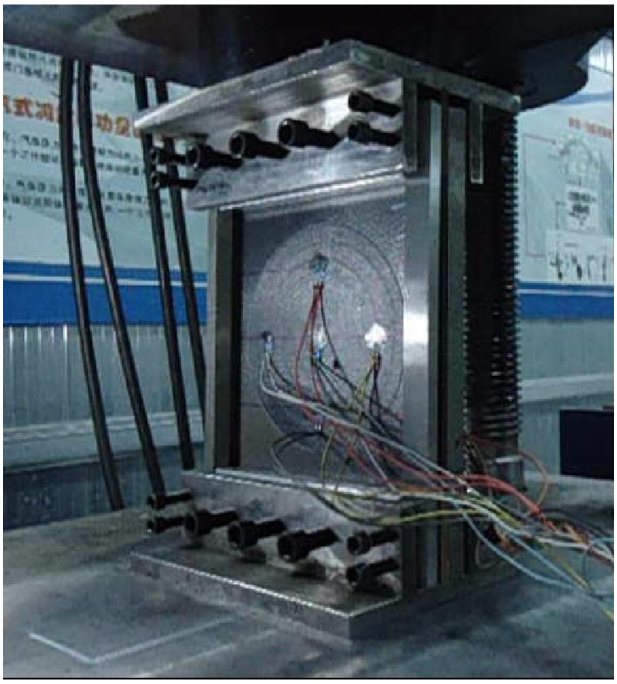

Fig. 2 Griped composite flush-repaired laminate specimen for compressive load experiment

3. FINITE ELEMENT ANALYSIS

3.1 Finite Element Mode and Strain Analysis

A 3-D finite element model was established by ABAQUS. Geometry, material and lay-up of the finite element model were the same as actual specimens. Each ply of actual specimens corresponded to a ply of 3-D solid element, and the material property of solid elements was defined according to the actual specimen material property and lay-up orientation per ply. Composite material was simulated with 3-D eight node hexahedron element (C3D8), while the adhesive was simulated with eight node bond ply element (C3D8) (Liu 2013).

Zero-thickness cohesive elements (COH3D8) was used between layers to simulate inter-laminar damage. The scarf joint flush-repaired finite element model was simplified as stepped-patch flush-repaired model to insert cohesive elements. Studies showed that the simplification could avoid stress singularity for base laminates and covering layers’ sharp edge at scarf joint flush-repaired slope angle during finite element analysis (Zhu 2012), besides, the mechanical property of flush-repaired composite laminate was almost the same before and after simplification.

To simulate the actual boundary condition of flush-repaired composite laminate specimens during experiments, the bottom face of laminates was fixed, and the external displacement freedom and rotate freedom in direction 1 and 2 of laminates' sides were constrained. The loaded top face of specimens had the loading direction freedom only. Then reference points were established and were constrained by distributed coupling constraint with all nodes on top face of specimens. In addition, all degrees of freedom between reference points and controlled region were constrained. Displacement load was applied on reference points, while displacement and force on reference points were recorded as output. Concrete boundary condition for flush-repaired composite laminates in finite element model is shown in Fig. 3.

Since specimens' compressive instability was a complex nonlinear process, there existed severe convergence problem when applying implicit solution method (Standard) in ABAQUS. To solve this problem, explicit solution method (Explicit) was applied to do quasi-static analysis during the loading process. Moreover, to simulate the buckling process of the specimens under compression with high fidelity, buckle method calculating instability mode was used first and then imperfection method was used to introduce structure initial deformation.

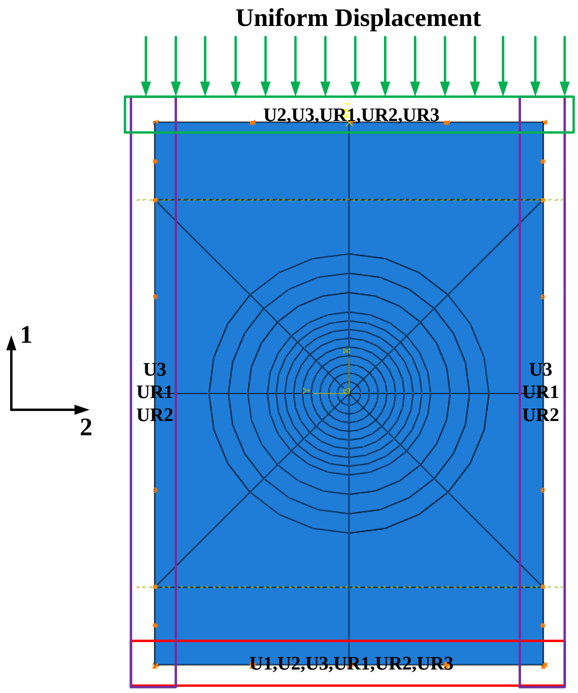

Fig. 3 Boundary conditions of the finite element model for composite flush-repaired laminates under compressive load

3.2 Failure Mode Analysis

Many failure criteria were established for composite laminates, such as stress-based, strain-based and energy-based failure criteria (Chrisxtos 1998). For bonding or bonding repair composite laminate failure, Guo (2012) adopted Cai-Wu failure criteria, Zhu (2012) and Wang (2011) adopted 3D Hashin failure criteria, while Liu (2013) and Yang (2012) adopted a differently approved 3D Hashin failure criteria. In this study, a 3D Hashin failure criteria was adopted to identify the damage of laminates on both the base laminate and the patch, after damage occurring material property reduction mode was applied to the base laminate and covering layers (Liu 2013). To calculate efficiently, damage of the laminates by contacting with the fixture was neglected.

As for failure criteria of adhesive between the base laminate and the patch, Guo (2012) adopted maximum strain criteria, Zhu (2012) and Wang (2011) adopted Ye criteria, Liu (2013) adopted secondary stress criteria, and Yang (2012) adopted maximum stress criteria. In this study, Ye criteria were applied to identify the adhesive failure, and the interface element failure criteria were referred to Guan (2012).

4. RESULTS AND DISCUSSION

4.1 Experimental Results

Failure loads on specimens of flush-repaired and virgin composite laminates under compressive load are listed in Table 3.

Table 3 Failure loads on specimens of composite laminate under compressive load

composite flush-repaired laminate specimen		virgin laminate specimen without any damage	
FY-1/kN	153.40	WY-1/kN	112.20
FY-2/kN	168.40	WY-2/kN	160.00
FY-3/kN	126.10	WY-3/kN	148.60
Average	149.30	Average	140.27

The load-stain curve of specimen FY-3 is shown in Fig. 4. With increased compressive load, the specimen began to buckle locally, and the strain became bifurcate obviously on the compressive cross of the specimens. The strain gauges on the compressive cross of the specimens can be divided into two groups. One group exhibited rising process indicating compressive strain decreased so that the compression degree of the specimens was weakened, corresponding to the tension face of the buckled specimens. The other group exhibited descending process indicating compressive strain increased so that the compressive degree of the specimens was aggravated, corresponding to the compressive face of the buckled specimens.

The bifurcation points on the load-strain curves of the specimens correspond to the buckling loads. Specimens’ buckling loads are listed in Table 4, in which n is the ratio of the failure load to the buckling load.

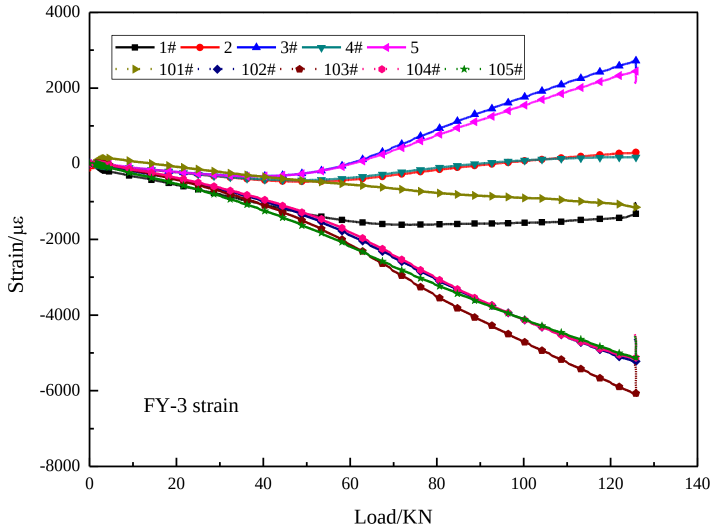

Fig. 4 Load-strain curves of No. FY-3 specimen

As shown in Table 4, the ratio of the average failure load to the average buckling load is 3.2 and 3.8 for flush-repaired and virgin composite laminate specimens, respectively. Thus, flush-repairing has a slight influence on post-buckling load-carrying capability of composite laminates under compressive load. That is slightly more serious than the flush-repairing influence on post-buckling load-carrying capability of composite laminates under shear load (Lan 2014).

Table 4 Buckling loads on specimens of composite laminate under compressive load

composite flush-repaired laminate specimen			virgin laminate specimen without any damage		
NO.	Buckling Load /kN	*n*	NO.	Buckling Load /kN	*n*
FY-1	48.00	3.2	WY-1	35.00	3.2
FY-2	54.00	3.1	WY-2	40.00	4.0
FY-3	40.00	3.2	WY-3	37.00	4.0
Average	47.33	3.2	Average	37.33	3.8

Compressive strength on flush-repaired composite laminate specimens is higher than that of virgin composite laminate specimens (Table 3 and Table 4). The ratio of the average failure load for the flush-repaired composite laminates to the virgin composite laminate specimens is 1.06, and ratio of the average buckling load is 1.27. This is similar to the influence of flush-repairing on composite laminate shear strength (Lan 2014). So the flush-repaired composite laminates recover the load-carrying capability well under compressive load, and the repaired laminates have better post-buckling load-carrying capability than the virgin laminates.

Failure modes for flush-repaired composite laminate specimens were all local buckling at non-repaired region (Fig. 5), and those for virgin laminate specimens were global buckling. The reason for the failure mode difference on composite laminate specimens before and after repairing was analyzed. Since thick covering layer resulted in higher local buckling loads at repaired region compared with those at non-repaired region, and hence as a result, the local buckling at non-repaired region occurred first and led to the final failure.

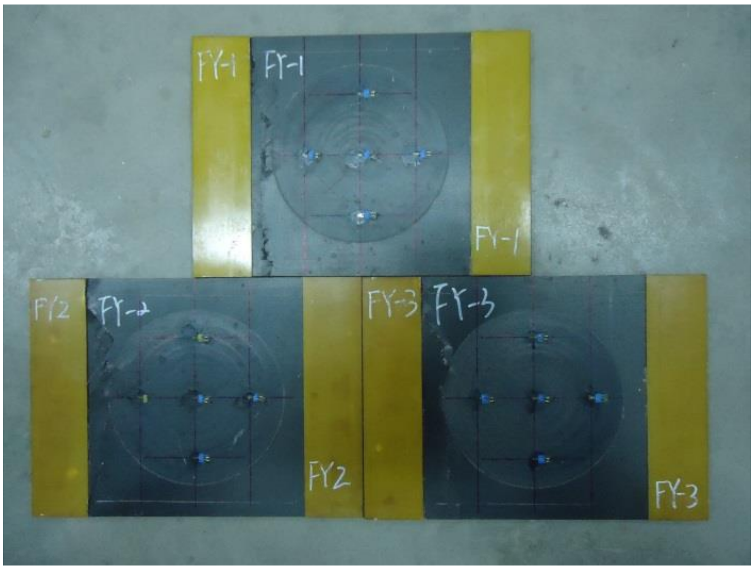

(a) Front view

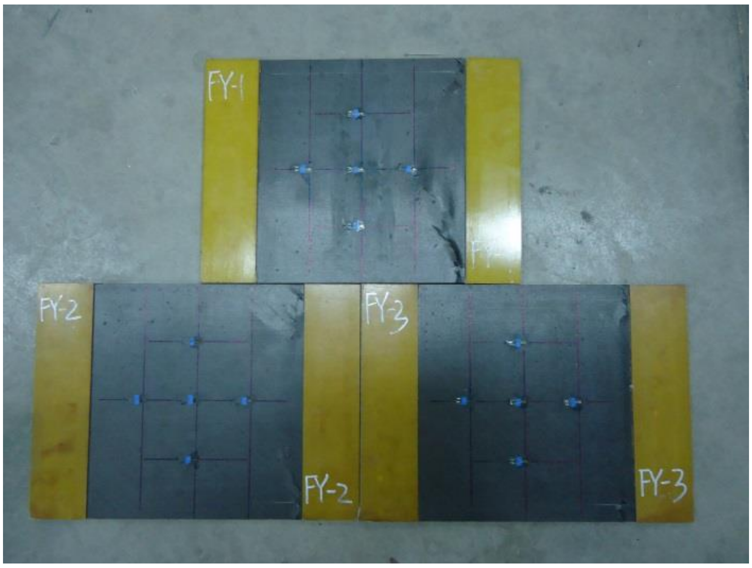

(b) Back view

Fig. 5 Failure mode of composite flush-repaired laminate specimens under compressive load

4.2 Finite element analysis results

The finite element analysis indicated that the failure load of flush-repaired composite laminates under compressive load was 141.89kN, 5.0% less than that from the experimental test.

The failure mode of the finite element analysis (Fig. 6) was the same as the experimental results with failure taking place at the non-repaired region. When the compressive load increasing near to the failure load, the composite laminate fiber damage occurred and the matrix cracked firstly, and then the fiber damage rapidly expanding led to the decrease of the global composite laminate load-carrying capability. Finally local buckling occurred at non-repaired region, while the patch covering-layer and adhesive were barely damaged.

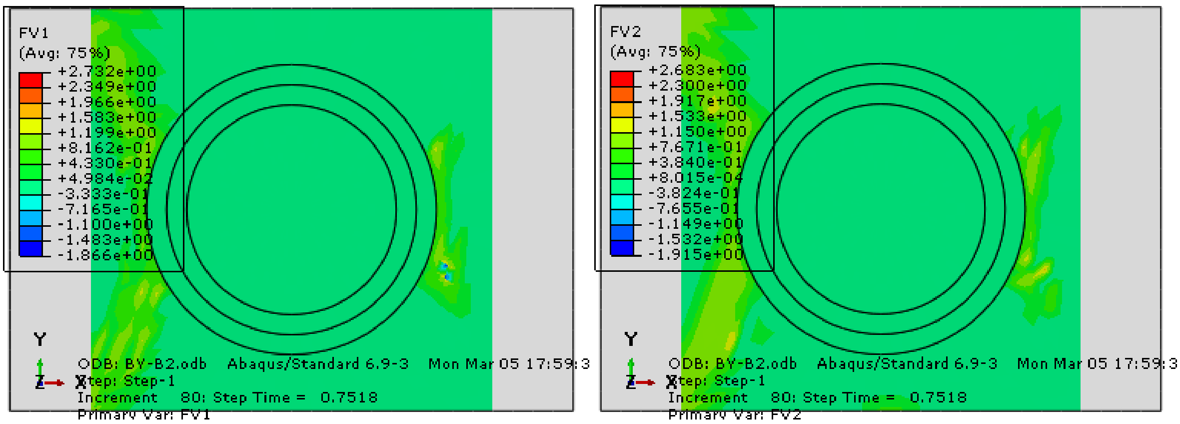

(a) Fiber failure moire pattern (b) Matrix failure moire pattern

Fig. 6 Failure mode of composite flush-repaired laminates finite element model under compressive load

5. CONCLUSIONS

The ratio of the average failure load for the flush-repaired composite laminates to the virgin composite laminate specimens is 1.06, and ratio of the average buckling load is 1.27. Flush-repaired composite laminates usually recover well under compressive load, and the repaired laminates have better post-buckling load-carrying capability than the virgin laminates. The failure mode for flush-repaired composite laminate specimens was local buckling at non-repaired region, and that for virgin laminate specimens was global buckling.

The finite element analysis showed that the failure load on flush-repaired composite laminates under compressive load was 141.89kN, 5.0% less than the experiment results. So the proposed finite element model is able to anticipate the failure mode and failure load of flush-repaired composite laminates under compressive load.

REFERENCES

Peng, J., Shi, J.(2008), "The Development Trend of Composite Materials for Large Aircraft Structure", *Aeronaut. Sci. Technol.*, **6**, 3-5.

Guo, X., Guan,Zh. D., Liu, S. (2012),"Tensile behavior and parameters designing of double-sides flush repair of composite laminates", *Acta Mater.Compos.Sin.*,**29**(1), 176-182.

Campilho, R. D. S. G., Moura, M. F. S. F., Domingues, J. J. M. S. (2007), "Stress and failure analysis of scarf repaired CFRP laminates using a cohesive damage mode",*J.Adhes. Sci. Technol.*, **21**(9): 855-870.

Zhu, Sh. H., Wang, Y. Q., Tong, M. B. (2012), "Progressive damage analysis on composite laminates stepped-patch adhesively bonding repair",*Acta Mater.Compos.Sin.*,**29**(6): 164-169.

Liu, S., Guan,Zh. D., Guo, X. (2013),"Tensile behavior of hybrid laminates repaired by full depth scarfing",*Acta Mater.Compos.Sin.*,**30**(1): 223-229.

Pen, X. W.(2016), "Research on Strength of Adhesive Bonded Composite Laminates" [D],NUAA.

Lan, Y. P., Xu.J. F., Du. K. (2014),"Experimental study and FEA on flush-repair of composite laminates under shear load",*Acta Mater.Compos.Sin.*,**31**(3): 803-808.

Soutis, C., Hu. F. Z. (2000),"Failure analysis of scarf-patch-repaired carbon fiber/ epoxy laminates under compression",*J. AIAA*, **38**(4): 737-740.

Yu, M., Xu, X. W. (2008), "Study of the compress strength of scarf patch repaired composite structures",*J. CUMT*, **37**(5): 709-714.

Xu, J. X., Cao, X. M., Li. D. H. (2011),"Research on stability of stiffened composite laminates with stepped-lap repair",*J.CAUC*, **29**(4): 1-3.

Chrisxtos, K. (1998),Yan, W. Y. Transl.(2011), "Design and analysis of composite structures with applications to aerospace structures",*Shanghai: SJTU Press*, 48-54.

Wang, Y. Q., Tong, M. B., Zhu, Sh. H. (2011),"Progressive damage analysis on adhesively bonding patch repair of composite laminates",*Acta Mater.Compos.Sin.*,**28**(3): 197-202.

Yang, Y. H., Zhou,Zh.G.,Guo, Y. (2012),"Effect of defects in the adhesive layer on strength of adhesively bonded single-lap composites joints",*Acta Mater.Compos.Sin.*,**29**(5): 157-163.

Guan.Zh. D., Li, Z. Sh., Liu, D. B. (2012),"Damage analysis of open-hole compression laminates",*Acta Mater.Compos.Sin.*,**29**(3): 167-172.